

Available online at [www.sciencedirect.com](http://www.sciencedirect.com)

ScienceDirect

journal homepage: [www.elsevier.com/locate/yexcr](http://www.elsevier.com/locate/yexcr)

## Research Article

# Mycophenolic acid mediated disruption of the intestinal epithelial tight junctions

Muhammad Qasim<sup>a,b</sup>, Hazir Rahman<sup>a,b</sup>, Raees Ahmed<sup>c</sup>, Michael Oellerich<sup>a</sup>, Abdul R. Asif<sup>a,\*</sup>

<sup>a</sup>Institute of Clinical Chemistry/UMG-Laboratories, University Medical Centre, Robert Koch Strasse 40, 37075 Goettingen, Germany

<sup>b</sup>Department of Microbiology, Kohat University of Science and Technology, 26000 Kohat, Pakistan

<sup>c</sup>Institute for Applied Science and Clinical Trials GmbH – IFS, Georg-August University, 37075 Goettingen, Germany

## ARTICLE INFORMATION

## Article Chronology:

Received 30 July 2013

Received in revised form

21 December 2013

Accepted 21 January 2014

Available online 7 February 2014

## Keywords:

Mycophenolic acid

Tight junctions

Myosin light chain 2

Permeability

## ABSTRACT

Gastrointestinal toxicity is a common adverse effect of mycophenolic acid (MPA) treatment in organ transplant patients, through poorly understood mechanisms. Phosphorylation of myosin light chain 2 (MLC2) is associated with epithelial tight junction (TJ) modulation which leads to defective epithelial barrier function, and has been implicated in GI diseases. The aim of this study was to investigate whether MPA could induce epithelial barrier permeability via MLC2 regulation. Caco-2 monolayers were exposed to therapeutic concentrations of MPA, and MLC2 and myosin light chain kinase (MLCK) expression were analyzed using PCR and immunoblotting. Epithelial cell permeability was assessed by measuring transepithelial resistance (TER) and the flux of paracellular permeability marker FITC-dextran across the epithelial monolayers. MPA increased the expression of MLC2 and MLCK at both the transcriptional and translational levels. In addition, the amount of phosphorylated MLC2 was increased after MPA treatment. Confocal immunofluorescence analysis showed redistribution of TJ proteins (ZO-1 and occludin) after MPA treatment. This MPA mediated TJ disruption was not due to apoptosis or cell death. Additionally ML-7, a specific inhibitor of MLCK was able to reverse both the MPA mediated decrease in TER and the increase in FITC-dextran influx, suggesting a modulating role of MPA on epithelial barrier permeability via MLCK activity. These results suggest that MPA induced alterations in MLC2 phosphorylation and may have a role in the patho-physiology of intestinal epithelial barrier disruption and may be responsible for the adverse effects (GI toxicity) of MPA on the intestine.

© 2014 Elsevier Inc. All rights reserved.

## Introduction

The tight junctions (TJs) are intercellular, multifunctional complexes present in the epithelial and endothelial cells which form the paracellular diffusion barrier [14,50]. This barrier contributes

to the regulation of epithelial permeability and intramembrane diffusion of ions and solutes through the paracellular space [5,30,58]. TJs are comprised of transmembrane (occludin, claudins and junctional adhesion molecules) and peripheral membrane proteins (zonula occludins [ZO-1], membrane-associated guanylate kinase,

\*Corresponding author. Fax: +49 55 1391 2505.

E-mail address: [asif@med.uni-goettingen.de](mailto:asif@med.uni-goettingen.de) (A.R. Asif).

and the Ras-related protein Rab13). These proteins interact with each other to form a complex protein network [54]. Various intestinal and non-intestinal disorders including inflammatory bowel disease, celiac disease, and diarrheal infections are characterized by barrier dysfunction which is thought to play a crucial role in their pathogenesis [5].

Mycophenolic acid (MPA) is the active agent in the two currently commercially available formulations: the MPA ester mycophenolate mofetil (MMF) and the enteric-coated salt mycophenolate sodium (EC-MS) [31]. After oral ingestion, MPA is liberated in the gastrointestinal tract, absorbed and metabolized in the liver to form MPA glucuronide (MPAG) and two other metabolites, 7-O-glucoside and acyl glucuronide (AcMPAG). AcMPAG is pharmacologically active and believed to be responsible for some MPA associated GI tract adverse effects [4]. MPA is an immunosuppressant which is frequently used for the prevention of acute transplant rejection. MPA is also used for the treatment of non-transplant, autoimmune, renal, rheumatological, gastrointestinal, ophthalmological, dermatological and neurological diseases [57]. Several immunosuppressive drugs including MPA used in solid organ transplantation lead to diarrhea [19]. Various possible aetiologies of this diarrhea have been described including infectious agents, drug reactions, metabolic alterations, and surgical complications. MPA has been claimed to account for 50% of all drug induced post-transplantation diarrhea [3], while 20% of total MPA complications involve the GI tract [19,38]. GI symptoms similar to those seen with Crohn's disease and enterocolitis are also observed in patients receiving MPA therapy [9,21,27,34,37]. The underlying mechanisms of MPA induced GI toxicity remain unclear; however, several hypotheses exist including direct toxicity as a result of its anti-proliferative effects, myelosuppression induced opportunistic infections, variations in local immune response, and AcMPAG adduct toxicity [19,55,56].

Several GI associated abnormalities, including inflammatory bowel disease (Crohn's disease and ulcerative colitis), and Graft versus host disease are characterized by epithelial barrier defects which contribute to increased intestinal permeability [8]. MLC phosphorylation is an important regulator of barrier function in health and disease [33]. Increased MLC phosphorylation leads to the rearrangement of TJ proteins (ZO-1, occludin, claudin-1 and claudin-4), disruption of perijunctional F-actin, and increases TJ permeability [8,52]. The key pathways associated with MLC phosphorylation are controlled either directly by MLCK activity or indirectly by Rho kinase mediated inhibition of phosphatase [2]. MLCK mediated MLC phosphorylation is sufficient to trigger downstream events necessary for barrier regulation and has a central role in many diseases that are characterized by intestinal barrier dysfunction (reviewed in [29]). The effects of MPA on cell junction's biophysical properties including paracellular permeability, and the regulation of TJ proteins, especially in relation to intestinal barrier defects, have not been well studied. Studies were conducted to explore the molecular effects of MPA on gut integrity via possible effects on TJs. We used Caco-2 cell monolayers as *in vitro* model of intestinal epithelia [1] and incubated them with therapeutic concentrations (3.1 mg/L, or 10  $\mu$ mol/L) of MPA. Trans-epithelial resistance (TER) measurements, paracellular influx assays, immunoblotting and immunofluorescence analyses were then conducted to evaluate integrity of the TJs complex. We hypothesized that MPA may modulate the TJs by altering expression and distribution of crucial TJs proteins via MLCK mediated MLC2 phosphorylation.

## Materials and methods

### Reagents

Reagents (and their sources) included agarose (Gibco BRL, Paisley, UK), magnesium chloride ( $MgCl_2$ ), M-MLV RT enzyme and 5 $\times$  buffer (Invitrogen, Karlsruhe, Germany), deoxynucleotide triphosphate (dNTP) (Roche, Mannheim, Germany), ribonuclease (RNAase) inhibitor (Promega, Mannheim, Germany), MPA, fluorescein isocyanate-dextran 4 kDa (FD4), 1-5-iodonaphthalene-1-sulfonyl-1H-hexahydro-1,4-diazepine hydrochloride (ML-7) and cytochalasin (CD) (Sigma-Aldrich, Mannheim, Germany), PCR primers (Eurofins, Ebersberg, Germany) and 10 $\times$  cell lysis buffer (Cell Signalling Technology, Danvers, MA, USA).

### Cell culture

The human colon adenocarcinoma cell line (Caco-2) was purchased from DSMZ (German collection of microorganisms and cell cultures, Braunschweig, Germany). Tissue culture media ingredients were obtained from PAA Laboratories (Pasching, Austria). Cells were grown in Dulbecco's modified Eagle's medium (DMEM) (4.5 g/L glucose) supplemented with 10% heat-inactivated fetal calf serum, 2 mmol/L glutamine, 50 IU/mL penicillin, 50 mg/mL streptomycin and non-essential amino acid supplement (1% v/v) under conditions of 37 °C, 5% CO<sub>2</sub> and 90% relative humidity. The Caco-2 cells were allowed to grow for 21 days of post-confluence to form differentiated and polarized monolayer growth [36]. The culture medium was changed every second day. DMSO at final concentration of 0.05% (v/v) was used as vehicle control in all experiment.

### LDH measurement

LDH measurements were performed using a commercially available LDH measurement kit (Roche, Mannheim, Germany) according to the manufacturer's instructions. This assay is based on the principle that LDH catalyzes the conversion of NADH (substrate) to NAD and the rate of this conversion is directly proportional to LDH activity. Briefly, cells were incubated in DMSO or 10  $\mu$ mol/L MPA for 72 h. Following incubation, supernatant medium was collected, centrifuged for 5 min at 15,700g at 4 °C and LDH was measured photometrically using a Hitachi analyzer (Roche, Mannheim, Germany). The experiments were repeated at least four times and values were represented as mean IU/L  $\pm$  SEM.

### Determination of caspase 3 activity

Cells were treated with DMSO or 10  $\mu$ mol/L MPA for 72 h and the caspase specific activity was measured using CaspACE™ Assay kits (Promega, WI, USA) as previously described [23]. Briefly, cell proteins (70  $\mu$ g) were mixed with reaction mixtures containing the colorimetric substrate Ac-DEVD-p-nitroaniline (Ac-DEVD-pNA). The pNA released from Ac-DEVD-pNA due to caspase activity was measured at a wavelength of 405 nm using an EL808 microplate reader (Bio-Tek instruments, VT, USA). Caspase 3 specific activity (CSA) in the cell extract was measured using the standard formula (CSA = pmol pNA liberated/h/ $\mu$ g protein). Five

independent experiments were performed and results were expressed as mean pmol pNA liberated/h/ $\mu$ g protein.

### Determination of trans-epithelial resistance (TER)

TER was measured as previously described [22]. Briefly, cells were seeded on polyester transwell inserts (6.5 mm diameter, 0.4  $\mu$ m pore size, 0.33 cm<sup>2</sup> growth area, Corning Costar Corporation, NY, USA) at  $2.0 \times 10^5$  cells/well and grown for 21 days post-confluence. Cells were treated in the apical side of the transwell inserts with DMSO, 10  $\mu$ mol/L MPA, or CD (10  $\mu$ mol/L) for 72 h or pre-treated with ML-7 (10  $\mu$ mol/L) for 1 h followed by 72 h treatment of MPA (10  $\mu$ mol/L) after cells developed into a differentiated and polarized monolayer. TER was measured using an EVOM voltohmmeter with a STX2 electrode (WPI, FL, USA). For epithelial resistance measurements, both the apical and basolateral sides of the epithelia were bathed in cell culture medium. Resistance (TER) =  $[RC - RE] \times A$ ; where RC is resistance of the cells ( $\Omega$ ); RE is resistance of the blank ( $\Omega$ ); and A is surface area of the membrane insert (cm<sup>2</sup>). TER was calculated as  $\Omega$  cm<sup>2</sup> for at least four consecutive measurements.

### FITC-dextran paracellular permeability

Epithelial permeability was assessed using a previously reported method [46,47]. Briefly, Caco-2 cells were grown into monolayers and treated as described above. Following treatment, cells were rinsed with PBS and incubated in Hank's balanced salt solution containing 1 mg/mL FITC-dextran 4 kDa (FD4) solution for 2 h. Permeability marker flux was assessed by taking 100  $\mu$ L from the basolateral chamber. Fluorescent signal was measured using a Lambda fluoro 320 fluorescence plate reader (MWG Biotech, Ebersberg, Germany) using 492 nm excitation and 520 nm emission filters. FD4 concentrations were determined using standard curves generated by serial dilution of FD4. Fluxes were calculated using the apparent permeability coefficient ( $P_{app}$ ) equation:  $P_{app} = [(\Delta C_A / \Delta t) V_A] / A \times C_L$ , where  $P_{app}$  is the apparent permeability (cm/s),  $\Delta C_A$  is the change of FD4 concentration, A is the surface area of the membrane (cm<sup>2</sup>),  $\Delta t$  is the change of time,  $V_A$  is the volume of the abluminal medium, and  $C_L$  is the initial concentration in the luminal chamber.

### RNA isolation, cDNA synthesis and real-time PCR

Total cellular RNA was extracted using the acid guanidinium-phenol-chloroform method (Trizol reagent; Invitrogen, CA) according to manufacturer's recommendations. Briefly, Caco-2 monolayers were scraped into Trizol reagent, homogenized, and RNA was extracted using chloroform/isopropanol precipitation. The precipitated RNA was dissolved in sterile water and stored at  $-80^\circ\text{C}$  until analysis. RNA concentration was determined with the GeneQuant II RNA/DNA calculator (Pharmacia Biotech, Freiburg, Germany) and quality was verified by OD<sub>260</sub>/OD<sub>280</sub> nm ratios and subsequent electrophoresis in 1.5% agarose gels using ethidium bromide staining. cDNA was synthesized from 2  $\mu$ g total RNA in a 30  $\mu$ L reaction mix containing  $1 \times$  RT-PCR buffer (10 mmol/L Tris-HCl [pH 8.3], 15 mmol/L KCl, 0.6 mmol/L MgCl<sub>2</sub>), 0.5  $\mu$ mol/L of each dNTP, 1 U/ $\mu$ L RNase inhibitor and 13.3 U/ $\mu$ L M-MLV RT enzyme. The RT reactions were performed in a thermocycler (Biometra, Goettingen, Germany) at  $75^\circ\text{C}$  for 5 min, and then  $42^\circ\text{C}$  for 1 h. cDNA was stored at  $-80^\circ\text{C}$  until use.

Primers for real time PCR were selected using the online Primer 3 software [41]. The primers used in this study were as follows: MLC2 (forward 5'-CAGGAGTCAAAGAGGCCTTCAAC-3', reverse 5'-CTG-TACAGCTCATCCACTTCTCA-3'); MLCK (forward 5'-CAACAGGGT-CACCAACCAGC-3', reverse 5'-GCCTTGCAGGTGTACTTGGC-3'); and elongation factor 2 (EF-2) (forward 5'-GACATCACCAAGGGTGTG-CAG-3', reverse 5'-GCGGTGACACTGGCATA-3'). Relative quantitative PCR was carried out using the LightCycler instrument (Roche, Mannheim, Germany). The total PCR volume of 20  $\mu$ L contained 1  $\mu$ L of cDNA solution, 2  $\mu$ L of  $10 \times$  PCR buffer (Invitrogen, Darmstadt, Germany), 2  $\mu$ L syber green, 1  $\mu$ L BSA, 1  $\mu$ L DMSO, 0.25  $\mu$ L of each primer (Eurofins MWG-Biotech AG, Ebersberg, Germany), 2.0 mmol/L MgCl<sub>2</sub>, 0.2 mmol/L of each dNTP, and 0.15 U/ $\mu$ L PAN Script DNA polymerase (PAN Biotech, Aidenbach, Germany). Amplification conditions were set to: MLC2 (initial denaturation 30 s at  $95^\circ\text{C}$ , repeated cycles of denaturation at  $95^\circ\text{C}$ , for 1 s, primer annealing at  $55^\circ\text{C}$  for 5 s, elongation at  $72^\circ\text{C}$  for 10 s, and fluorescence reading at  $82^\circ\text{C}$ ), and MLCK (initial denaturation for 30 s at  $95^\circ\text{C}$  and repeated cycles of denaturation at  $95^\circ\text{C}$  for 1 s, primer annealing at  $60^\circ\text{C}$  for 5 s, elongation at  $72^\circ\text{C}$  for 10 s, and fluorescence reading at  $82^\circ\text{C}$ ). ROCK (initial denaturation for 30 s at  $95^\circ\text{C}$  and repeated cycles of denaturation at  $95^\circ\text{C}$  for 1 s, primer annealing at  $60^\circ\text{C}$  for 5 s, elongation at  $72^\circ\text{C}$  for 10 s, and fluorescence reading at  $80^\circ\text{C}$ ), and EF-2 (initial denaturation for 30 s at  $95^\circ\text{C}$ , repeated cycles of denaturation at  $95^\circ\text{C}$ , for 1 s, primer annealing ( $55^\circ\text{C}$ , 5 s), elongation ( $72^\circ\text{C}$ , 10 s), and fluorescence reading at  $88^\circ\text{C}$ ). For each sample, real-time PCR reactions were performed in quadruplicate. RNA relative expression was calculated as fold change using the comparative threshold cycle ( $C_T$ ) method ( $2^{-\Delta\Delta C_T}$ ) [49] with EF-2 used as the internal control gene. The relative expression of mRNA in the treated samples was determined as a fold increase compared with control samples. The PCR product was run on 1.5% agarose gel electrophoresis to confirm the specificity of the amplified product.

### Immunoblotting

Caco-2 cells were rinsed with ice-cold PBS and lysed with lysis buffer-CS (50 mM Tris/HCl, pH 7.4, 1.0% Triton X-100, 5 mM EGTA, 10 mM sodium fluoride, 2  $\mu$ g/mL leupeptin, 10  $\mu$ g/mL aprotinin, 10  $\mu$ g/mL bestatin, 10  $\mu$ g/mL pepstatin A, 1 mM vanadate and 1 mM PMSF). Cell lysate was centrifuged and total cell proteins (clear supernatant) were separated. Protein contents were measured using the Bio-Rad protein assay kit (Bio-Rad Laboratories) according to vendor instructions. Protein lysates were separated by SDS-PAGE and blotted onto PVDF (Immobilon, Millipore, MA, USA) using the Trans-Blot SD cell system (Bio-rad, Munich, Germany) for 30 min at 15 V in a blotting buffer (192 mmol/L glycine, 20% methanol, and 25 mmol/L Tris [pH 8.3]). The membranes were blocked with 5% (w/v) milk in TBS-T buffer (50 mmol/L Tris-HCl [pH 7.5], 200 mmol/L NaCl, 0.05% Tween 20) for 1 h at room temperature followed by washing twice in TBS-T for 5 min. The membranes were incubated with a 1: 500 dilution of a mouse monoclonal anti-MLC antibody (Sigma, Mannheim, Germany), 1: 10,000 dilution of mouse monoclonal anti-MLCK antibody (Sigma, Mannheim, Germany), 1: 1000 rabbit anti-phospho MLC antibody (Cell Signaling, Beverly, USA), 1  $\mu$ g/mL rabbit anti-ZO-1, 0.5  $\mu$ g/mL mouse anti-occludin (Zymed, CA, USA), or 1: 5000 anti- $\beta$  actin (Sigma, Mannheim, Germany) in 5% BSA in TBS-T overnight at  $4^\circ\text{C}$ . Following washing in TBS-T,

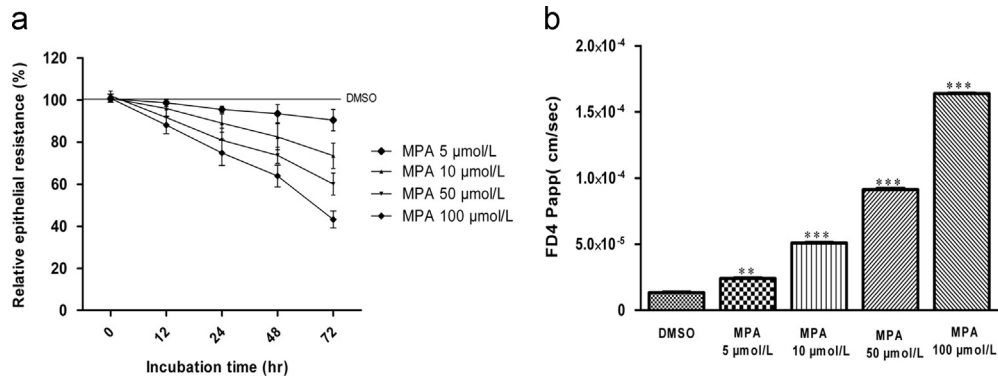


**Fig. 1 – Effect of MPA treatment on TER and FD4 permeability of Caco-2 cell monolayers.** Caco-2 cells were cultured on filter inserts and grown for 21 days post-confluence to form differentiated monolayers. (a) Caco-2 cells were treated with MPA (5–100 µmol/L) for 0–72 h. MPA concentration and time dependent decrease in TER were observed. Graph shows relative epithelial resistance versus time (h) with means ± SEM from four independent experiments. (b) Paracellular flux of FD4. Values are means of apparent permeability for FD4 (cm/s) which is the amount of apical FD4 crossing the insert membrane per cm<sup>2</sup>/s. Bars show SEM and \*\* =  $p < 0.005$  and \*\*\* =  $p < 0.0005$ .

membranes were then incubated with appropriate HRP-conjugated secondary antibodies (Bio-Rad, Munich, Germany). The membranes were washed with PBS and prepared for enhanced chemiluminescence (GE, Buckinghamshire, UK) according to the manufacturer's instructions. Developed membranes were then exposed to hyperfilm-ECL (GE, Buckinghamshire, UK). The films were scanned and protein band densities were quantified with the Lab Image software, version 2.71 (Kapelan, Leipzig, Germany).

### Immunofluorescence microscopy of TJ proteins

Cell monolayers were grown on Lab-Tek™ eight chamber slides (Nunc, Naperville, IL, USA) and treated as indicated above. Cells were immunolabelled as previously described [11] with some modifications. Briefly, cells were rinsed with PBS and fixed in 3.7% formaldehyde at room temperature for 20 min. Cell monolayers were then rinsed in PBS and permeabilized in 0.2% Triton X-100 for 7 min at room temperature. Cells were rinsed in PBS followed by blocking with 1% bovine serum albumin (BSA) for 30 min at room temperature. Cells were incubated with 3 µg/mL anti-rabbit ZO-1 and 2 µg/mL anti-mouse occludin (Zymed, San Francisco, USA) overnight at 4 °C. After washing with PBS, cells were incubated with anti-rabbit IgG conjugated to Alexa 488 and anti-mouse IgG conjugated to cydye 3 (Molecular Probes, Eugene, OR, USA) in 1% BSA for 1 h at room temperature. For F-actin localization cells were incubated in 0.33 µg/mL of FITC-conjugated phalloidin (Sigma-Aldrich, St. Louis, USA) in PBS for 30 min as described previously [40]. Cells were also incubated with DAPI (Molecular Probes, Eugene, USA) for 10 min to stain nuclei. After washing with PBS, cells were mounted using the Dako fluorescence mounting medium (Dako, Carpinteria, USA) and stored at 4 °C in dark until analyzed. The fluorescence was visualized using Axiovert 200M confocal microscope (Carl Zeiss, Jena, Germany). All of the fluorescent labeling experiments were repeated four times to ensure reproducibility.

### Statistics

The data are presented as sample means with error bars indicating the standard error of the mean. The  $p$  value was calculated

using Student's  $t$  test and a  $p$  value  $< 0.05$  was considered statistically significant.

## Results

### MPA altered TER and TJs permeability in a concentration and time dependant manner

In the present study, the effect of MPA on Caco-2 TJ integrity was determined by measuring TER and epithelial permeability to the paracellular marker FD4. To assess the influence of MPA treatment on TER, cells were incubated with different concentrations of MPA (5–100 µmol/L) for up to 72 h. DMSO did not have any significant effect on TER of polarized Caco-2 cell monolayers. Increasing concentrations of MPA exhibited concentration- and time-dependant decreases in Caco-2 TER (Fig. 1a). The mean TER decreased by about 10%, 27% and 41% after 5, 10 and 50 µmol/L MPA treatment respectively. The maximal decrease (57%) in TER was observed at 100 µmol/L MPA concentration. The decrease in Caco-2 TER increased with time between 12 h and 72 h (Fig. 1a).

Similarly, MPA was associated with a concentration-dependent increase in Caco-2 paracellular permeability to FD4 (Fig. 1b). FD4 permeability analysis following 72 h MPA treatment showed a concentration-dependant increase in FD4 influx. The FD4 influx from the apical to the basolateral chamber was increased 1.5, 2.7, 4.6, and 7.9 fold after incubation with 5, 10, 50, and 100 µmol/L MPA concentrations respectively (Fig. 1b).

### MPA mediated increase in permeability was not due to cell death/apoptosis

To determine whether MPA induced decreases in TER and increased FD4 permeability were due to TJ proteins modulation and not due to the cell death, the LDH release from the treated cells was determined. LDH measurement has previously been used as an indicator of cell death [25]. Exposure to 10 µmol/L MPA for 72 h did not result in any significant increase in LDH release from the Caco-2 cells (Fig. 2a). Furthermore, caspase 3 activity

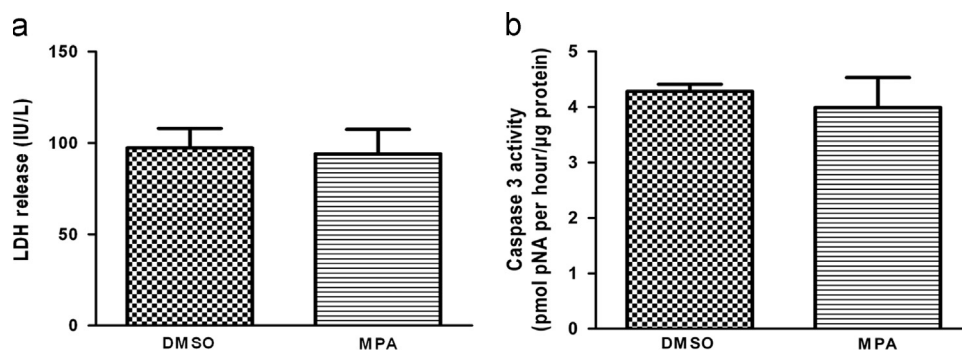


**Fig. 2 – Effect of MPA on cell viability and apoptosis in Caco-2 cells.** Caco-2 were grown for 21 days post-confluence and treated with DMSO or MPA (10  $\mu\text{mol/L}$ ) for 72 h. (a) Cell viability was assessed by measuring the lactate dehydrogenase (LDH) release in the culture media. Data represent IU/L LDH released into the media per h/ $\mu\text{g}$  protein. (b) Apoptosis was determined by measuring the caspase-3 activity in cell lysates using CaspACE™ Assay kits. Caspase 3 activity is expressed as pmol/h/ $\mu\text{g}$ . Values are presented as the mean  $\pm$  SEM; of four independent experiments and the significance was determined by Student's *t*-test.

was measured to check the effect of MPA on cell apoptosis. 10  $\mu\text{mol/L}$  MPA exposures for 72 h did not cause any significant apoptosis as compared to DMSO (vehicle) (Fig. 2b). These findings suggest that the TJs disruption caused by MPA was not associated with cell death or apoptosis.

#### MPA increased the expression of MLC2 and MLCK in Caco-2 cells

In a previous study we reported that MPA increased the total MLC2 expression in HEK-293 cells [39]. Additionally, we observed up-regulation of MLCK and ROCK expressions by MPA in HEK-293 and HT-29 cells (data not shown). In view of these findings, we investigated regulation of MLC2 expression and MLCK in Caco-2 cells. MLCK is involved in the regulation of barrier function through the phosphorylation of MLC2 in response to diverse stimuli [62,63]. In line with the previous findings [39], MPA treatment increased the expression of MLC2 at both the mRNA (1.5 fold increase) and protein levels (1.47 fold increase) in Caco-2 cells (Fig. 3a and b). MLCK expression was also up-regulated by MPA (10  $\mu\text{mol/L}$ ) at the mRNA (1.9 fold) and protein levels (2.1 fold) (Fig. 3a and b). To analyze for the possible involvement of MLCK in the MPA mediated TJs disruption, we determined the effect of MPA on total protein expression of MLC2 and MLCK in the presence of ML-7 (Fig. 3b). ML-7 acts as a selective antagonist of MLCK by competing for its ATP binding site and reverses the effects of agents involved in TJs disruptions [24]. Previously, it was reported that ML-7 had no significant effect on total MLC2 and MLCK expression and that ML-7 mainly affects the phosphorylation of MLC2 by decreasing the activity of MLCK [25]. In the present study, expressional analysis showed that MPA treatment in the presence of ML-7 did not alter total MLC2 and MLCK expression, which was observed after MPA treatment alone (Fig. 3b).

#### MPA-mediated increase in MLC phosphorylation through MLCK

MLC phosphorylation has been extensively studied with regard to tight junction regulation and has been reported to be required for increased paracellular permeability [52,62]. To determine whether MPA caused any defect in the epithelial barrier through

phosphorylation of MLC2, we checked the phosphorylation of MLC2 by immunoblotting using specific phospho-MLC2 antibody. MPA treatment (10  $\mu\text{mol/L}$ ) for 72 h increased the expression of phospho-MLC2 by 2.8 fold (Fig. 4). Previously it was shown that ML-7 inhibits MLCK driven MLC2 phosphorylation by inhibiting MLCK activity [24,25]. We observed that the presence of ML-7 in the medium was able to reverse the effect of MPA on MLC2 phosphorylation (Fig. 4). To further validate these results, cells were incubated with CD which is an actin-disrupting drug that has previously been reported to increase MLC2 phosphorylation [15]. Our results also showed that CD increased phospho-MLC2 expression (Fig. 4), which is consistent with the previous report [15].

#### MLCK inhibition partially prevented MPA effects on TER and permeability

To investigate whether MPA mediated TJs alteration is through effects on MLCK, we pre-treated Caco-2 monolayers with ML-7 for 1 h and then co-incubated them with (10  $\mu\text{mol/L}$ ) MPA for the indicated time periods. It was previously reported that ML-7 prevents TJs disrupting agent mediated decreases in TER and increases the FD4 permeability via inhibition of MLCK [24,62]. Co-treatment with ML-7 and MPA resulted in a significant higher TER as compared to cells treated with MPA alone (Fig. 5a). Similarly, apical to basal FD4 influx was also reduced in cells co-treated with MPA and ML-7 (Fig. 5b). CD was previously reported to decrease TER and increase permeability [48]. In the following experiments, similar to MPA, CD treated cells showed significant decreases in TER and increases in FD4 influx (Fig. 5a and b). These findings suggest that the MPA-induced increases in Caco-2 TJ permeability are at least partly the result of a mechanism closely associated with MLCK expression and activity.

#### MPA modulated Caco-2 F-actin distribution

The perijunctional ring of F-actin is the fundamental unit of the actin cytoskeleton that supports the tight junction and thus plays an important role in barrier regulation [26]. Structural alterations of the F-actin-based cytoskeleton are used to detect changes in actin and tight junctions [24,67]. To investigate whether MPA

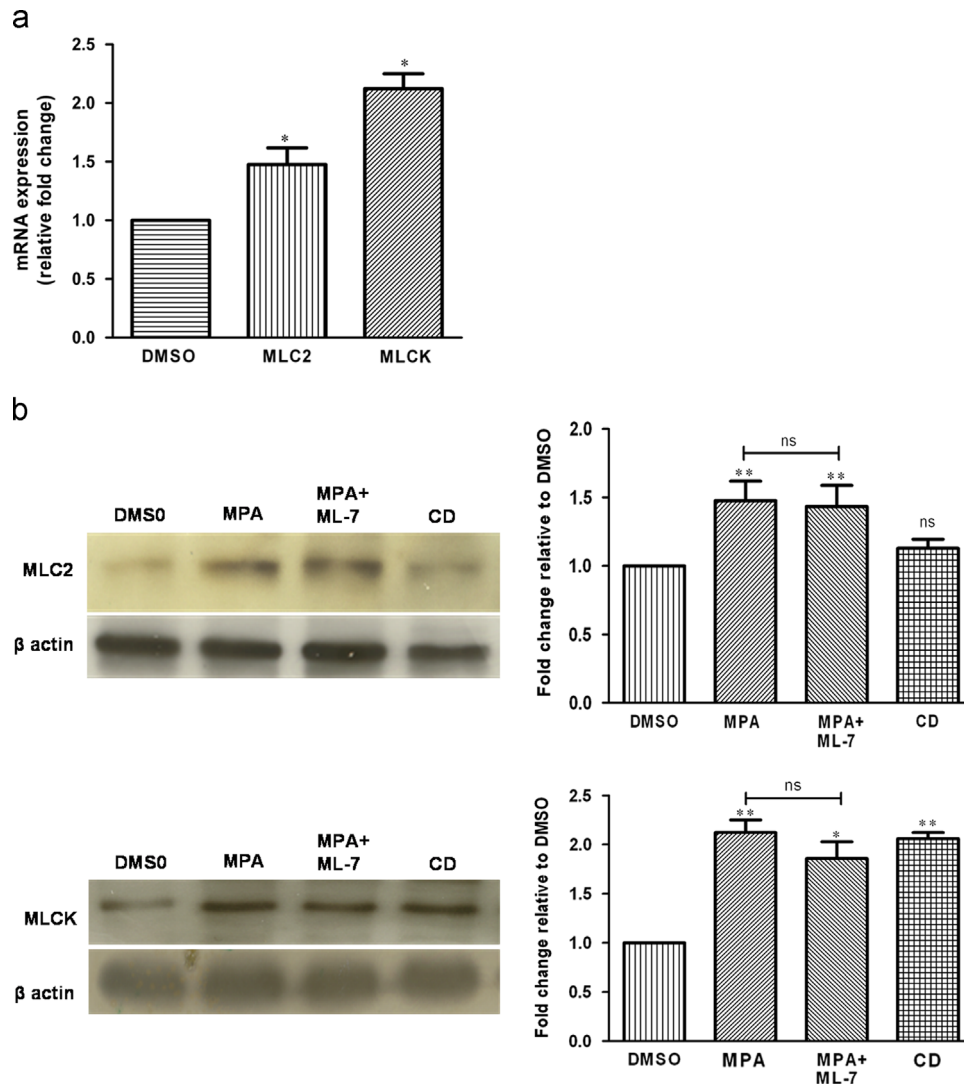


**Fig. 3 – Effect of MPA on MLC2 and MLCK expression in Caco-2 cells.** Caco-2 monolayers (21 days post-confluence) were incubated with either vehicle (DMSO), MPA (10  $\mu\text{mol/L}$ ), MPA (10  $\mu\text{mol/L}$ )+ML-7 (10  $\mu\text{mol/L}$ ), or CD (10  $\mu\text{mol/L}$ ) for 72 h. (a) mRNA expression analysis for MLC2, and MLCK. Total RNA was extracted, reverse transcribed and subjected to real-time PCR analysis. EF-2 was used as a house keeping gene and the relative mRNA expression of MLC2 and MLCK in the MPA and DMSO (vehicle) treated samples was determined using the comparative threshold cycle ( $C_T$ ) method ( $2^{-\Delta\Delta C_T}$ ) as described in Material and methods section. Data indicate the mean of four independent experiments  $\pm$  SEM. (b) Immunoblot analyses for MLC2 and MLCK. Whole cell lysates were resolved on 1DE and immunoblotted using MLC2 and MLCK specific antibodies.  $\beta$  actin was used as a control for an equal amount of protein load. Densitometric analysis was done using the Lab image software. The data represent mean relative intensities  $\pm$  SEM from four independent immunoblots. \* $p < 0.05$  and \*\* $p < 0.005$  significance relative to DMSO.

mediated colonic epithelial barrier disruption was associated with structural modulation of the F-actin cytoskeleton; we stained Caco-2 cells with FITC-labelled phalloidin, a commonly used fluorescent marker for F-actin [24,40]. In the vehicle control (DMSO) cell monolayers, the F-actin cytoskeleton was uniformly organized as shown in Fig. 6a–c. Following 72 h exposure to 10  $\mu\text{mol/L}$  of MPA (Fig. 6d–f), the uniform distribution of actin staining in epithelial cells appeared disrupted and was marked by randomly distributed dense patches of staining, which suggest that the disruption of the actin cytoskeleton could be a possible mechanism for the alterations in the TJs functions following MPA treatment.

### Inhibition of MLCK prevented MPA mediated redistribution of TJ proteins

The modulatory effect of MPA on TJs proteins, ZO-1 and occludin was investigated by immunofluorescent labeling. Changes in the distribution and expression of occludin and ZO-1 can be used as the markers for determination of TJs disruption which has been implicated in several GI tract diseases [20,45]. Confocal analyses of ZO-1 and occludin distribution showed uniform and continuous staining at the plasma membrane in control cells (DMSO) (Fig. 7a–c). MPA treatment (10  $\mu\text{mol/L}$ ) for 72 h led to redistribution of ZO-1 and occludin proteins. The most prominent features

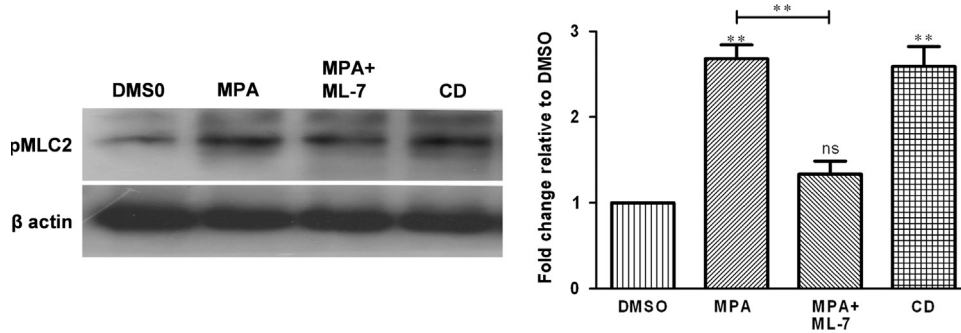


Fig. 4 – Effect of ML-7 on MPA-mediated increases MLC phosphorylation. Caco-2 monolayers (21 days post-confluent) were incubated with either vehicle (DMSO), MPA (10  $\mu\text{mol/L}$ ), MPA (10  $\mu\text{mol/L}$ )+ML-7 (10  $\mu\text{mol/L}$ ), or CD (10  $\mu\text{mol/L}$ ) for 72 h. Total cell proteins were isolated and equal amount of protein was loaded resolved on 1DE. Expression was analyzed by immunoblot analysis using antibodies against p-MLC2.  $\beta$  actin was used as a control for an equal amount of protein load. Bands were quantified using the Lab image software. The data represent the mean of 4 independent experiments  $\pm$  SEM. \*\*= $p < 0.005$  and ns indicates statistically not significant value.

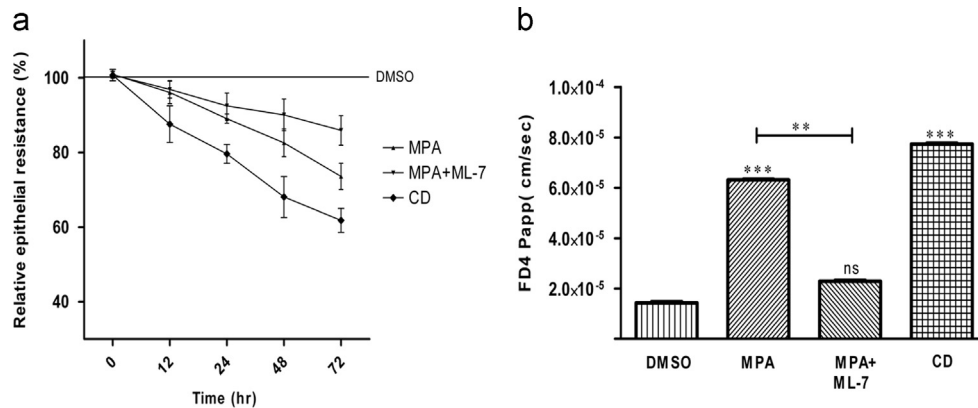


Fig. 5 – ML-7 co-treatment reversed the effect of MPA on TER and permeability. Cells were grown to 21 days post-confluence and incubated with DMSO, MPA (10  $\mu\text{mol/L}$ ), MPA (10  $\mu\text{mol/L}$ )+ML-7 (10  $\mu\text{mol/L}$ ), or CD (10  $\mu\text{mol/L}$ ) for 72 h. The effects on (a) TER and (b) FD4 influx were measured as described in Material and methods section. ML-7 (a specific MLCK inhibitor) prevented both the MPA-mediated increase in FD4 paracellular diffusion and the decreases in TER. Data are the mean  $\pm$  SEM of at least four independent experiments. \*\*= $p < 0.005$  and \*\*\*= $p < 0.0005$ .

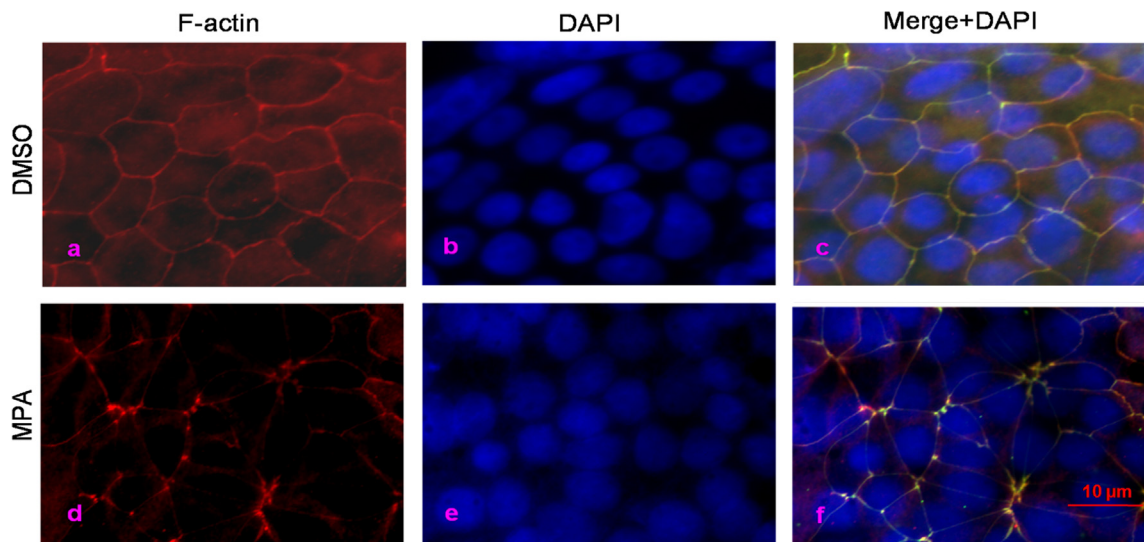
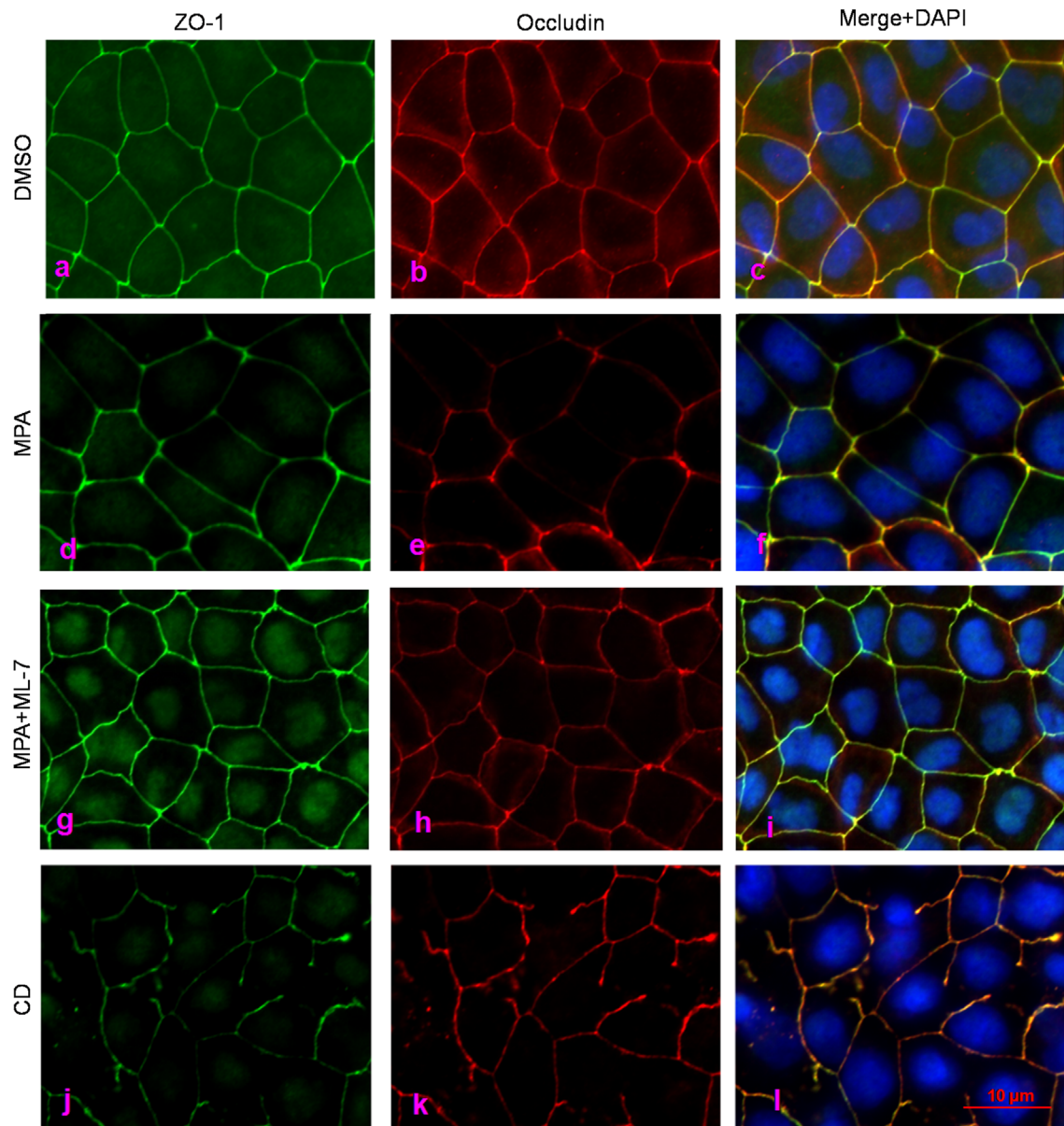


Fig. 6 – MPA induced remodeling of the F-actin cytoskeleton. Caco-2 cells grown to 21 days post-confluence followed by 72 h treatment with DMSO (a–c), or 10  $\mu\text{mol/L}$  MPA (d–f). Cells were fixed, permeated, and F-actin was stained with FITC-phalloidin (red) and nuclei were stained with DAPI (blue), as described in Material and methods section. Fluorescence images were obtained using an Axiovert 200M confocal microscope. Images are representative of 4 independent experiments.



**Fig. 7** – Effect of ML-7 co-treatment with MPA on distribution of TJ proteins (ZO-1 and occludin). Caco-2 cells were grown for 21 days post-confluence and treated with either vehicle (DMSO), MPA (10  $\mu\text{mol/L}$ ), MPA (10  $\mu\text{mol/L}$ )+ML-7 (10  $\mu\text{mol/L}$ ), or CD (10  $\mu\text{mol/L}$ ) for 72 h. Cells were fixed, permeated, and stained for ZO-1 and occludin, as described in Materials and methods section. The figure shows the distribution of ZO-1 and occludin in Caco-2 cells exposed to DMSO (vehicle) (a–c) or MPA (d–f), MPA+ML-7 (g–i), and CD (j–l). Cells were double stained for ZO-1 (a, d, g, and j) and occludin (b, e, h, and k). An overlay (ZO-1, occludin, and DAPI) is shown in the right panel (c, f, i, and l). Corresponding proteins were detected with secondary antibodies conjugated with either FITC 488 (green; ZO-1) or cy3 (red; occludin). DAPI (blue; nuclei) was used to stain nuclei. Images were examined using confocal microscopy. Images presented are representative images of 5 independent experiments.

were disappearance of staining at the cellular periphery, with aggregation and paracellular openings between the adjacent cells (Fig. 7 d–f). These microscopic alterations at the apical cellular borders correlated with the amount of increased TJ permeability (Fig. 1) observed. Previously, it was reported that the redistribution of TJ proteins by TJ disrupting agents can be reversed by inhibiting MLCK [51,60,68]. Immunofluorescence localization of occludin and ZO-1 showed that ML-7 could partly prevent the redistribution of ZO-1 and occludin induced by MPA exposure

(Fig. 7g–i) when compared to cells treated with MPA alone (Fig. 7d–f). ML-7 co-treatment induced reassembly of the ZO-1 and occludin at the cellular borders with reclosure of the paracellular gaps. The MPA induced disruption of TJ proteins distribution was prevented by an MLCK inhibitor (ML-7), indicating that the downstream alteration of TJ proteins is dependent on MLCK activation. In contrast, CD, like MPA, disrupts the distribution of ZO-1 and occludin as shown by disappearance of these proteins from the paracellular membrane (Fig. 7j–l).

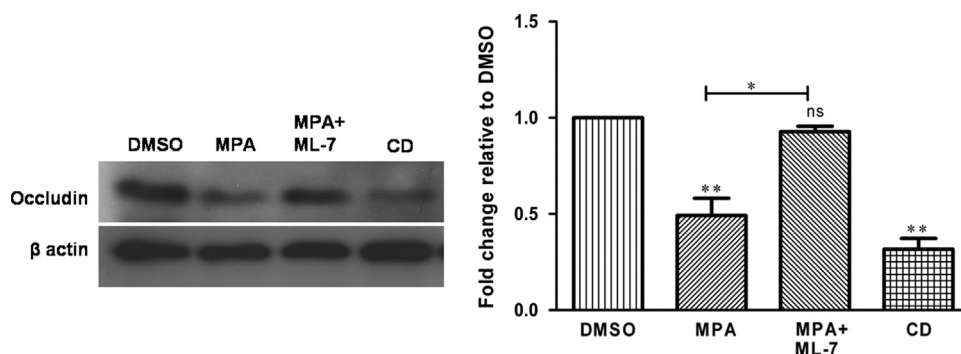


**Fig. 8 – Effect of ML-7 co-treatment with MPA on occludin protein expression in Caco-2 cells.** Caco-2 cell monolayers following 21 days post-confluency were incubated with DMSO, MPA (10  $\mu\text{mol/L}$ )+ML-7 (10  $\mu\text{mol/L}$ ) or CD (10  $\mu\text{mol/L}$ ) for 72 h. Protein extracts were immunoblotted for occludin and  $\beta$ -actin. Densitometric measurement was done with the Lab image software. Values are means  $\pm$  SEM ( $n=4$ ). \*\*= $p<0.005$ .

### Inhibition of MLCK prevented MPA mediated down regulation of occludin protein expression

We further investigated whether MPA quantitatively altered the expression of TJs protein (occludin) in Caco-2 cells. Immunoblot analysis showed that 10  $\mu\text{mol/L}$  of MPA decreased the expression of occludin by 2.1 fold (Fig. 8). These expressional changes are consistent with the immunostaining of occludin protein which also revealed disappearance and redistribution of occludin protein from the membranes (Fig. 7). ML-7 was able to reverse the effect of MPA on occludin expression by increasing its expression by 1.92 fold as compared to cells treated with MPA alone. CD treatment showed a 3.2 fold decrease in occludin protein as compared to DMSO control (Fig. 8).

## Discussion

Intestinal cells form a crucial physical and functional barrier, which regulates the movement of water, electrolytes, nutrients, and xenobiotics [53]. The gastrointestinal tract is directly involved in the metabolism and transport of various endogenous and exogenous compounds [12]. Several intestinal diseases are characterized by barrier dysfunction including inflammatory bowel disease, graft versus host disease, and infectious enterocolitis (reviewed in [6]). It has been previously reported that epithelial barrier defects lead to increased intestinal permeability and the development of diarrhea in human patients with bowel diseases [13] and in mouse models [6]. MPA associated gastrointestinal adverse effects are a major concern in transplantation medicine and diarrhea is the most frequent unwanted clinical outcome following treatment with MPA regimes [10]. Previous reports showed that MPA is associated with gastrointestinal mucosal injury [9,32,34,35,37]. The effect of therapeutic concentrations of MPA on the gastrointestinal epithelial barrier is not well described. Diverse physiological and pathophysiological stimuli cause intestinal barrier dysfunction, regulated via several pathways such as those involving protein kinase C, protein kinase A, MLCK, Rho-kinase, mitogen-activated protein kinases, and phosphoinositide 3-kinase. Disturbances in these pathways can all lead to the alteration in TJs protein expression and distribution [5,17]. In a previous study, we observed a significant increase in the MLC2

expression in HEK-293 cells following MPA exposure [39]. MLC2 phosphorylation via MLCK and/or ROCK has been implicated in several barrier disorders [15]. To better understand the possible mechanism of MPA mediated TJs regulation, we used Caco-2 monolayers as a colonic model [44]. The present study demonstrates for the first time in vitro that MPA, at non-toxic and therapeutic concentrations produces a significant modulation of intestinal epithelial barrier function in Caco-2 cells. The Caco-2 cell line is widely used as an in vitro intestinal barrier cell model, which exhibits a well differentiated brush border, TJs, and intestinal proteins [44,64]. In the present study we observed that MPA exposure increased TJs permeability and impaired TJ proteins (ZO-1 and occludin) expression and distribution. On the other hand, the MPA concentrations used did not cause significant apoptosis or cell death, suggesting that the effects of MPA on GI barrier function are the result of a non-cytotoxic mechanism.

Previously it was shown that MLCK activity in Caco-2 cells triggers a series of molecular processes such as induction of MLC phosphorylation, myosin- $\text{Mg}^{2+}$ -ATPase activation, and perijunctional actin-myosin interaction which are responsible for actin filament disruption leading to Caco-2 epithelial barrier opening [24]. Several agents increase MLCK mediated MLC2 phosphorylation which disrupts TJ proteins, leading to the increased TJs permeability implicated in barrier associated diseases [52]. We investigated the possible disruptive role of MPA on epithelial barrier permeability and attempted to link this effect with MLCK-induced MLC-2 phosphorylation.

To demonstrate the effect of MPA on barrier properties of this colonic model, Caco-2 cells were exposed to non-cytotoxic concentrations of MPA (10  $\mu\text{mol/L}$ ) followed by measurements of TER and influx of markers. Determination of TER and influx of permeability markers are widely used techniques to assess the integrity and permeability of monolayers [65] because TJs disruption can be reflected by the reduction in TER and the increase in influx of permeability markers [7].

Our data revealed that MPA increased Caco-2 cell monolayer permeability as shown by decreases in TER and increases in FD4 influx (Fig. 1). These findings are in agreement with another report on the effects of MMF (an ester prodrug of MPA) on the barrier function of small bowel and distal colon of Wistar rats [28].

TJs proteins, ZO-1, and occludin are protein markers which are widely used to investigate TJs integrity [16,52]. These proteins maintain structure and function of TJs integrity which are vital for

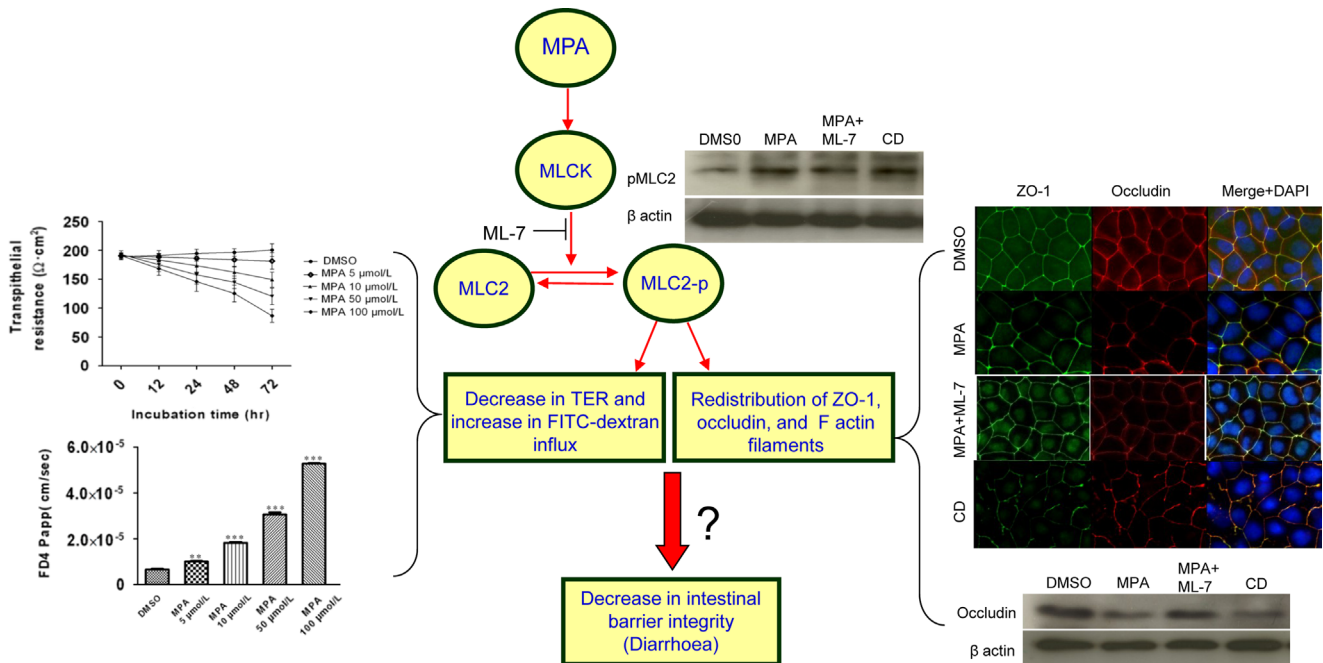


**Fig. 9 – Proposed model of MPA mediated TJ disruption.** MPA increased the MLCK-mediated MLC2 phosphorylation in Caco-2 cells monolayers. MLC-2 phosphorylation alters the expression and distribution of TJ proteins (ZO-1 and occludin) and has been identified as a key factor in development of barrier defects in several intestinal diseases. MLC-2 phosphorylation also alters the distribution of F actin filaments and the associated TJ disruption results in decrease in TER and increased in paracellular influx. In the present study we observed that MPA disrupted TJ, characterized by increased MLCK expression, and MLC2 phosphorylation. We therefore propose that MPA associated TJ disturbance is dependent on MLCK-driven MLC phosphorylation that leads to decreased expression and redistribution of TJ proteins. Pre-treatment of ML-7 (a specific inhibitor of MLCK) partially prevented the MPA mediated increased in MLC2 phosphorylation, disturbance of TJ proteins, and increase in permeability. We hypothesized that the observed increase in paracellular permeability following MPA treatment is due to TJ disruption caused by MLC2 phosphorylation, which mediates alterations in the expression and distribution of TJ proteins. Thus the results of the above events could be responsible for GI toxicity observed in some patients on MPA therapy.

normal intestinal architecture [43,50]. The disturbance in the distribution and expression of these proteins has been observed in intestinal barrier disorders [7,8]. In the present study, we investigated the effect of MPA on the distribution and expression of ZO-1 and occludin. We found that exposure of Caco-2 monolayers (21-days post-confluency) to therapeutic, non-cytotoxic concentrations of MPA for 72 h led to a decrease in the expression of occludin proteins, as evidenced by Western blot analysis (Fig. 8). Under normal conditions ZO-1 and occludin are generally present at the pericellular boundary, and distributed homogeneously, presenting a characteristic feature of intact TJs structure. Disruption and redistribution of TJs proteins have been reported previously in several studies that suggested that alteration in these proteins can lead to hyperpermeability [52,66]. MLCK mediated MLC-2 phosphorylation (involved in modulation of ZO-1 and occludin morphologically and biochemically) can induce an increase in TJs permeability [52]. Furthermore, we also demonstrated that MPA exposure change the distribution of ZO-1 and occludin proteins, as revealed by a discontinuous pattern of immunofluorescent staining of these TJs proteins (Fig. 7). To investigate whether MLCK was involved in MPA modulation of TJs, we used a specific MLCK inhibitor, ML-7 which is a selective antagonist of MLCK [42]. Previously it was reported that inhibition of MLCK mediated MLC phosphorylation by ML-7 can prevent or reverse TJs barrier losses induced by several agents such as TNF $\alpha$ ,

cytochalasin B, and ethanol [18,24,25,62]. To investigate the effect of MPA on MLCK activity, we pre-incubated cell monolayers with ML-7 followed by MPA exposure. Results showed that ML-7 could at least partially reverse the MPA mediated decrease in TER as well as the increase in FD4 influx. ML-7 was able to prevent the MPA induced redistribution of ZO-1 and occludin (Fig. 7). Additionally, ML-7 significantly decreased the expression of occludin protein (Fig. 8). Treatment with CD, a known stimulant of MLCK and actin-depolymerising agent [15] which was used as positive control for the effects of MPA treatment, also showed a decrease in TER and increase in paracellular flux (Fig. 5). Previously, it was reported that CD was able to increase MLCK activity and MLC2 phosphorylation [15], which our results confirmed. In addition, we found that CD was able to alter the expression and distribution of TJs proteins which is consistent with results of a previous study of CD treated epithelial cells [59]. These results showed that both CD and MPA decreased TER and disrupted the actin cytoskeleton.

The present study revealed that inhibition of MLCK activity by ML-7 significantly prevented the MPA mediated increase in MLC2 phosphorylation with no significant effect on total MLCK and MLC2 expression.

MLC2 phosphorylation has a key role in maintaining TJs integrity by regulating actomyosin contraction [62]. Several pathways were described previously which regulate the phosphorylation of MLC2;

among them Rho-kinase and MLCK signaling are widely studied in the context of barrier defects [61]. MLCK is involved in the regulation of barrier function by phosphorylation of MLC2 in response to diverse stimuli [62,63]. ML-7 via MLCK inhibition prevents the disruption of both occludin and actin, which demonstrates the importance of MLCK activity in TJs physiology [60]. Our results suggest that increases in MLCK might be responsible for the MPA induced redistribution of ZO-1 and occludin in Caco-2 monolayers.

In conclusion, the present study indicates for the first time that MPA at therapeutic concentrations produce functional alterations in TJs of Caco-2 cells resulting in abnormal TJs permeability, and redistribution of TJs proteins including displacement of F-actin. While requiring further investigation, MLCK inhibition by ML-7 significantly reduced the effect of MPA exposure on TJs disruption, thus suggesting a pivotal role of MLCK in regulating TJs barrier properties (Fig. 9). These findings provide new insights into the mechanism by which therapeutic use of MPA may alter intestinal epithelial barrier functions and suggest mechanisms which may be responsible for some of the GI adverse effects especially the diarrhea associated with MPA. Further in-depth studies are needed to explore the mechanisms involved in adverse consequences of MPA mediated disruption of TJs,

### Funding support

M. Qasim and H. Rahman were funded by the Human Resource Development Program of HEC, Pakistan and the Kohat University of Science and Technology, Kohat, Pakistan.

### Conflict of interest

The authors declare that they have no conflict of interest.

### Acknowledgments

We gratefully acknowledge Prof. Dr. Uwe Groß and Prof. Dr. Stefanie Pöggeler for their ideas and advice. In addition, we are thankful to Christina Wiese, Susanne Goldmann, Christa Scholz, Reiner Andaq, and Ulrike Bonitz for the expert technical assistance. Special thanks to Prof. Dr. Gabor Kottra for providing us the TER instrument and Prof. Dr. Giuliano Ramadori for the access to the immunofluorescence microscope facility. We are also very thankful to Prof. Dr. P. Walson for the proof reading of the manuscript.

### REFERENCE

- [1] X. Alvarez-Hernandez, G.M. Nichols, J. Glass, Caco-2 cell line: a system for studying intestinal iron transport across epithelial cell monolayers, *Biochim. Biophys. Acta (BBA) – Biomembr.* 1070 (1991) 205–208.
- [2] J.M. Anderson, C.M. Van Itallie, Tight junctions and the molecular basis for regulation of paracellular permeability, *Am. J. Physiol.* 269 (1995) G467–G475.
- [3] H. Arslan, E.K. Inci, O.K. Azap, H. Karakayali, A. Torgay, M. Haberal, Etiologic agents of diarrhea in solid organ recipients, *Transpl. Infect. Dis.* 9 (2007) 270–275.
- [4] N.A.K.B. Bullingham, R.E. Clinical, Pharmacokinetics of mycophenolate mofetil, *Clin. Pharmacokinet.* 34 (1998) 425–455.
- [5] R.M. Catalioto, C.A. Maggi, S. Giuliani, Intestinal epithelial barrier dysfunction in disease and possible therapeutic interventions, *Curr. Med. Chem.* 18 (2011) 398–426.
- [6] D.R. Clayburgh, T.A. Barrett, Y. Tang, J.B. Meddings, L.J. Van Eldik, D.M. Watterson, L.L. Clarke, R.J. Mrsny, J.R. Turner, Epithelial myosin light chain kinase-dependent barrier dysfunction mediates T cell activation-induced diarrhea in vivo, *J. Clin. Invest.* 115 (2005) 2702–2715.
- [7] D.R. Clayburgh, T.A. Barrett, Y. Tang, J.B. Meddings, L.J. Van Eldik, D.M. Watterson, L.L. Clarke, R.J. Mrsny, J.R. Turner, Epithelial myosin light chain kinase-dependent barrier dysfunction mediates T cell activation-induced diarrhea in vivo, *J. Clin. Invest.* 115 (2005) 2702–2715.
- [8] D.R. Clayburgh, L. Shen, J.R. Turner, A porous defense: the leaky epithelial barrier in intestinal disease, *Lab. Invest.* 84 (2004) 282–291.
- [9] I.J. Dalle, B.D. Maes, K.P. Geboes, W. Lemahieu, K. Geboes, Crohn's-like changes in the colon due to mycophenolate?, *Colorectal Dis.* 7 (2005) 27–34.
- [10] N.M. Davies, J. Grinyo, R. Heading, B. Maes, H.U. Meier-Kriesche, M. Oellerich, Gastrointestinal side effects of mycophenolic acid in renal transplant patients: a reappraisal, *Nephrol. Dial. Transpl.* 22 (2007) 2440–2448.
- [11] V. Dodane, K.M. Amin, J.R. Merwin, Effect of chitosan on epithelial permeability and structure, *Int. J. Pharm.* 182 (1999) 21–32.
- [12] C. Duggan, J. Gannon, W.A. Walker, Protective nutrients and functional foods for the gastrointestinal tract, *Am. J. Clin. Nutr.* 75 (2002) 789–808.
- [13] S.P. Dunlop, J. Hebden, E. Campbell, J. Naesdal, L. Olbe, A.C. Perkins, R.C. Spiller, Abnormal intestinal permeability in subgroups of diarrhea-predominant irritable bowel syndromes, *Am. J. Gastroenterol.* 101 (2006) 1288–1294.
- [14] M.G. Farquhar, G.E. Palade, Junctional complexes in various epithelia, *J. Cell Biol.* 17 (1963) 375–412.
- [15] L.M. Feighery, S.W. Cochrane, T. Quinn, A.W. Baird, D. O'Toole, S.E. Owens, D. O'Donoghue, R.J. Mrsny, D.J. Brayden, Myosin light chain kinase inhibition: correction of increased intestinal epithelial permeability in vitro, *Pharm. Res.* 25 (2008) 1377–1386.
- [16] M. Furuse, M. Itoh, T. Hirase, A. Nagafuchi, S. Yonemura, S. Tsukita, S. Tsukita, Direct association of occludin with ZO-1 and its possible involvement in the localization of occludin at tight junctions, *J. Cell Biol.* 127 (1994) 1617–1626.
- [17] L. Gonzalez-Mariscal, R. Tapia, D. Chamorro, Crosstalk of tight junction components with signaling pathways, *Biochim. Biophys. Acta* 1778 (2008) 729–756.
- [18] S.R. Guntaka, G. Samak, A. Seth, N.F. Larusso, R. Rao, Epidermal growth factor protects the apical junctional complexes from hydrogen peroxide in bile duct epithelium, *Lab. Invest.* 91 (2011) 1396–1409.
- [19] J.H. Helderman, S. Goral, Gastrointestinal complications of transplant immunosuppression, *J. Am. Soc. Nephrol.* 13 (2002) 277–287.
- [20] S. Jain, T. Suzuki, A. Seth, G. Samak, R. Rao, Protein kinase C  $\zeta$  phosphorylates occludin and promotes assembly of epithelial tight junctions, *Biochem. J.* 437 (2011) 289–299.
- [21] H.C. Kim, S.B. Park, Mycophenolate mofetil-induced ischemic colitis, *Transpl. Proc.* 32 (2000) 1896–1897.
- [22] B.A. Koeneman, Y. Zhang, P. Westerhoff, Y. Chen, J.C. Crittenden, D.G. Capco, Toxicity and cellular responses of intestinal cells exposed to titanium dioxide, *Cell Biol. Toxicol.* 26 (2010) 225–238.
- [23] P. Levy, H. Robin, F. Bertrand, M. Kornprobst, J. Capeau, Butyrate-treated colonic Caco-2 cells exhibit defective integrin-mediated signaling together with increased apoptosis and differentiation, *J. Cell. Physiol.* 197 (2003) 336–347.

- [24] T.Y. Ma, N.T. Hoa, D.D. Tran, V. Bui, A. Pedram, S. Mills, M. Merryfield, Cytochalasin B modulation of Caco-2 tight junction barrier: role of myosin light chain kinase, *Am. J. Physiol. Gastrointest. Liver Physiol.* 279 (2000) G875–G885.
- [25] T.Y. Ma, D. Nguyen, V. Bui, H. Nguyen, N. Hoa, Ethanol modulation of intestinal epithelial tight junction barrier, *Am. J. Physiol.* 276 (1999) G965–G974.
- [26] J.L. Madara, J.R. Pappenheimer, Structural basis for physiological regulation of paracellular pathways in intestinal epithelia, *J. Membr. Biol.* 100 (1987) 149–164.
- [27] B.D. Maes, I. Dalle, K. Geboes, M. Oellerich, V.W. Armstrong, P. Evenepoel, B. Geypens, D. Kuypers, M. Shipkova, K. Geboes, Y.F. Vanrenterghem, Erosive enterocolitis in mycophenolate mofetil-treated renal-transplant recipients with persistent afebrile diarrhea, *Transplantation* 75 (2003) 665–672.
- [28] M. Malinowski, P. Martus, J.F. Lock, P. Neuhaus, M. Stockmann, Systemic influence of immunosuppressive drugs on small and large bowel transport and barrier function, *Transpl. Int.* 24 (2011) 184–193.
- [29] A.M. Marchiando, W.V. Graham, J.R. Turner, Epithelial barriers in homeostasis and disease, *Annu. Rev. Pathol.* 5 (2010) 119–144.
- [30] K. Matter, M.S. Balda, Signalling to and from tight junctions, *Nat. Rev. Mol. Cell Biol.* 4 (2003) 225–236.
- [31] N. Newbold, B. Riley, K. Hardiner, A review of enteric-coated mycophenolate sodium for renal transplant immunosuppression, *Clin. Med.: Ther.* 1 (2009) 927–933.
- [32] T. Nguyen, J.Y. Park, J.R. Scudiere, E. Montgomery, Mycophenolic acid (cellcept and myofortic) induced injury of the upper GI tract, *Am. J. Surg. Pathol.* 33 (2009) 1355–1363.
- [33] A. Nusrat, M. Giry, J.R. Turner, S.P. Colgan, C.A. Parkos, D. Carnes, E. Lemichez, P. Boquet, J.L. Madara, Rho protein regulates tight junctions and perijunctional actin organization in polarized epithelia, *Proc. Natl. Acad. Sci.* 92 (1995) 10629–10633.
- [34] J.C. Papadimitriou, C.B. Cangro, A. Lustberg, A. Khaled, J. Nogueira, A. Wiland, E. Ramos, D.K. Klassen, C.B. Drachenberg, Histologic features of mycophenolate mofetil-related colitis: a graft-versus-host disease-like pattern, *Int. J. Surg. Pathol.* 11 (2003) 295–302.
- [35] J.R. Parfitt, S. Jayakumar, D.K. Driman, Mycophenolate mofetil-related gastrointestinal mucosal injury: variable injury patterns, including graft-versus-host disease-like changes, *Am. J. Surg. Pathol.* 32 (2008) 1367–1372.
- [36] M.D. Peterson, M.S. Mooseker, Characterization of the enterocyte-like brush border cytoskeleton of the C2BBE clones of the human intestinal cell line, Caco-2, *J. Cell Sci.* 102 (1992) 581–600.
- [37] U.P. Phatak, P. Seo-Mayer, D. Jain, M. Selbst, S. Husain, D.S. Pashankar, Mycophenolate mofetil-induced colitis in children, *J. Clin. Gastroenterol.* 43 (2009) 967–969.
- [38] C. Ponticelli, P. Passerini, Gastrointestinal complications in renal transplant recipients, *Transpl. Int.* 18 (2005) 643–650.
- [39] M. Qasim, H. Rahman, M. Oellerich, A. Asif, Differential proteome analysis of human embryonic kidney cell line (HEK-293) following mycophenolic acid treatment, *Proteome Sci.* 9 (2011) 57.
- [40] G. Ranaldi, I. Marigliano, I. Vespignani, G. Perozzi, Y. Sambuy, The effect of chitosan and other polycations on tight junction permeability in the human intestinal Caco-2 cell line(1), *J. Nutr. Biochem.* 13 (2002) 157–167.
- [41] S.H. Rozen, S. Primer3, on the WWW for general users and for biologist programmers, *Methods Mol. Bio.* 132 (2000) 365–386.
- [42] M. Saitoh, T. Ishikawa, S. Matsushima, M. Naka, H. Hidaka, Selective inhibition of catalytic activity of smooth muscle myosin light chain kinase, *J. Biol. Chem.* 262 (1987) 7796–7801.
- [43] S.Y. Salim, J.D. Soderholm, Importance of disrupted intestinal barrier in inflammatory bowel diseases, *Inflamm. Bowel Dis.* 17 (2011) 362–381.
- [44] Y. Sambuy, I. De Angelis, G. Ranaldi, M.L. Scarino, A. Stamatii, F. Zucco, The Caco-2 cell line as a model of the intestinal barrier: influence of cell and culture-related factors on Caco-2 cell functional characteristics, *Cell Biol. Toxicol.* 21 (2005) 1–26.
- [45] N. Sawada, M. Murata, K. Kikuchi, M. Osanai, H. Tobioka, T. Kojima, H. Chiba, Tight junctions and human diseases, *Med. Electron Microsc.* 36 (2003) 147–156.
- [46] N. Schlegel, S. Burger, N. Golenhofen, U. Walter, D. Drenckhahn, J. Waschke, The role of VASP in regulation of cAMP- and Rac 1-mediated endothelial barrier stabilization, *Am. J. Physiol.: Cell Physiol.* 294 (2008) C178–C188.
- [47] N. Schlegel, M. Meir, V. Spindler, C.T. Germer, J. Waschke, Differential role of Rho GTPases in intestinal epithelial barrier regulation in vitro, *J. Cell. Physiol.* 226 (2011) 1196–1203.
- [48] M. Schliwa, Action of cytochalasin D on cytoskeletal networks, *J. Cell Biol.* 92 (1982) 79–91.
- [49] T.D. Schmittgen, K.J. Livak, Analyzing real-time PCR data by the comparative C(T) method, *Nat. Protoc.* 3 (2008) 1101–1108.
- [50] E.E. Schneeberger, R.D. Lynch, The tight junction: a multi-functional complex, *Am. J. Physiol.: Cell Physiol.* 286 (2004) C1213–C1228.
- [51] K.G. Scott, J.B. Meddings, D.R. Kirk, S.P. Lees-Miller, A.G. Buret, Intestinal infection with *Giardia* spp. reduces epithelial barrier function in a myosin light chain kinase-dependent fashion, *Gastroenterology* 123 (2002) 1179–1190.
- [52] L. Shen, E.D. Black, E.D. Witkowski, W.I. Lencer, V. Guerriero, E.E. Schneeberger, J.R. Turner, Myosin light chain phosphorylation regulates barrier function by remodeling tight junction structure, *J. Cell Sci.* 119 (2006) 2095–2106.
- [53] M. Shimizu, Interaction between food substances and the intestinal epithelium, *Biosci. Biotechnol. Biochem.* 74 (2010) 232–241.
- [54] K. Shin, V.C. Fogg, B. Margolis, Tight junctions and cell polarity, *Annu. Rev. Cell Dev. Biol.* 22 (2006) 207–235.
- [55] M. Shipkova, V.W. Armstrong, M. Oellerich, E. Wieland, Acyl glucuronide drug metabolites: toxicological and analytical implications, *Ther. Drug Monit.* 25 (2003) 1–16.
- [56] M. Shipkova, V.W. Armstrong, M. Oellerich, E. Wieland, Mycophenolate mofetil in organ transplantation: focus on metabolism, safety and tolerability, *Expert Opin. Drug Metab. Toxicol.* 1 (2005) 505–526.
- [57] P.M. Stassen, C.G. Kallenberg, C.A. Stegeman, Use of mycophenolic acid in non-transplant renal diseases, *Nephrol. Dial. Transpl.* 22 (2007) 1013–1019.
- [58] E. Steed, M.S. Balda, K. Matter, Dynamics and functions of tight junctions, *Trends Cell Biol.* 20 (2010) 142–149.
- [59] B.R. Stevenson, D.A. Begg, Concentration-dependent effects of cytochalasin D on tight junctions and actin filaments in MDCK epithelial cells, *J. Cell Sci.* 107 (1994) 367–375.
- [60] V.S. Subramanian, J.S. Marchant, D. Ye, T.Y. Ma, H.M. Said, Tight junction targeting and intracellular trafficking of occludin in polarized epithelial cells, *Am. J. Physiol.: Cell Physiol.* 293 (2007) C1717–C1726.
- [61] S. Terry, M. Nie, K. Matter, M.S. Balda, Rho signaling and tight junction functions, *Physiology* 25 (2010) 16–26.
- [62] J.R. Turner, B.K. Rill, S.L. Carlson, D. Carnes, R. Kerner, R.J. Mrsny, J.L. Madara, Physiological regulation of epithelial tight junctions is associated with myosin light-chain phosphorylation, *Am. J. Physiol.* 273 (1997) C1378–C1385.
- [63] J.R. Turner, E.D. Black, J. Ward, C.M. Tse, F.A. Uchwat, H.A. Alli, M. Donowitz, J.L. Madara, J.M. Angle, Transepithelial resistance can be regulated by the intestinal brush-border Na<sup>+</sup>/H<sup>+</sup> exchanger NHE3, *Am. J. Physiol.: Cell Physiol.* 279 (2000) C1918–C1924.
- [64] R.B. van Breemen, Y. Li, Caco-2 cell permeability assays to measure drug absorption, *Expert Opin. Drug Metab. Toxicol.* 1 (2005) 175–185.
- [65] C.H. von Bonsdorff, S.D. Fuller, K. Simons, Apical and basolateral endocytosis in Madin–Darby canine kidney (MDCK) cells grown on nitrocellulose filters, *EMBO J.* 4 (1985) 2781–2792.

- 
- [66] F. Wang, W.V. Graham, Y. Wang, E.D. Witkowski, B.T. Schwarz, J.R. Turner, Interferon-gamma and tumor necrosis factor-alpha synergize to induce intestinal epithelial barrier dysfunction by up-regulating myosin light chain kinase expression, *Am. J. Pathol.* 166 (2005) 409–419.
- [67] L.f. Xu, C. Xu, Z.Q. Mao, X. Teng, L. Ma, M. Sun, Disruption of the F-actin cytoskeleton and monolayer barrier integrity induced by PAF and the protective effect of ITF on intestinal epithelium, *Arch. Pharm. Res.* 34 (2011) 245–251.
- [68] D. Yu, A.M. Marchiando, C.R. Weber, D.R. Raleigh, Y. Wang, L. Shen, J.R. Turner, MLCK-dependent exchange and actin binding region-dependent anchoring of ZO-1 regulate tight junction barrier function, *Proc. Natl. Acad. Sci. USA* 107 (2010) 8237–8241.